Inactivation and Pharmacological Properties of sqKv1A Homotetramers in *Xenopus* Oocytes Cannot Account for Behavior of the Squid "Delayed Rectifier" K^+ Conductance

Henry H. Jerng and William F. Gilly
Hopkins Marine Station, Pacific Grove, California 93950 USA

ABSTRACT Considerable published evidence suggests that α-subunits of the cloned channel sqKv1A compose the "delayed rectifier" in the squid giant axon system, but discrepancies regarding inactivation properties of cloned versus native channels exist. In this paper we define the mechanism of inactivation for sqKv1A channels in *Xenopus* oocytes to investigate these and other discrepancies. Inactivation of sqKv1A in *Xenopus* oocytes was found to be unaffected by genetic truncation of the N-terminus, but highly sensitive to certain amino acid substitutions around the external mouth of the pore. External TEA and K^+ ions slowed inactivation of sqKv1A channels in oocytes, and chloramine T (Chl-T) accelerated inactivation. These features are all consistent with a C-type inactivation mechanism as defined for *Shaker* B channels. Treatment of native channels in giant fiber lobe neurons with TEA or high K^+ does not slow inactivation, nor does Chl-T accelerate it. Pharmacological differences between the two channel types were also found for 4-aminopyridine (4AP). SqKv1A's affinity for 4AP was poor at rest and increased after activation, whereas 4AP block occurred much more readily at rest with native channels than when they were activated. These results suggest that important structural differences between sqKv1A homotetramers and native squid channels are likely to exist around the external and internal mouths of the pore.

INTRODUCTION

Studies of voltage-gated ion channels in the squid giant axon have contributed to fundamental discoveries such as the basis of action potential generation (Hodgkin and Huxley, 1952), the mechanism of open-channel block (Armstrong, 1969), and the existence of gating currents (Armstrong and Bezanilla, 1973). Although single channel studies have revealed three species of voltage-gated K^+ channels in the giant axon (Llano et al., 1988) and its cell bodies in the giant fiber lobe (GFL) of the stellate ganglion (Nealey et al., 1993), the vast majority of the classic, "delayed-rectifier" K^+ conductance (g_K) in this system has been attributed to a 20 pS channel (Llano and Bookman, 1986; Perozo et al., 1991; Nealey et al., 1993).

Heterologous expression of a squid cDNA (sqKv1A) isolated from the stellate-ganglion/GFL complex produces K^+ channels in *Xenopus* oocytes with macroscopic and single channel properties similar to those of the native 20 pS channel (Rosenthal et al., 1996). These biophysical data, along with localization of sqKv1A transcripts and protein in the giant-axon/GFL system, strongly support the hypothesis that channels formed by sqKv1A α-subunits underlie the native macroscopic g_K. This assignment is also supported by the pH-dependence for block of both channel types by tityustoxin-Kα (Ellis et al., 2001). This feature in sqKv1A is accounted for by titration of a single histidine residue in the external turret region.

Submitted November 6, 2001, and accepted for publication February 15, 2002.

Address reprint requests to W. F. Gilly, Hopkins Marine Station, Pacific Grove, CA 93950. Tel.: 831-655-6220; Fax: 831-655-6220; E-mail: lignje@stanford.edu.

0006-3495/02/06/3022/15 $2.00

Although such a stringent set of matches reasonably justifies identification of sqKv1A as a component of the native channel, it does not demonstrate that native channels are composed of sqKv1A homotetramers or address whether sqKv1A α-subunits experience different post-translational modifications in the two cases. Functional effects in these cases might be subtle, and the exceptional ability to study native g_K in squid axons and GFL neurons permits a detailed examination of this fundamental issue.

In this paper we focus on three important functional discrepancies that exist between sqKv1A channels expressed in *Xenopus* oocytes and native g_K in giant axons and GFL neurons. First, external TEA and K^+ ions slow inactivation of sqKv1A channels in oocytes (see also Brock et al., 2001) in essentially the same way as that described for classic C-type inactivation of *Shaker* B (Choi et al., 1991; Lopez-Barneo et al., 1993; Baukrowitz and Yellen, 1995) and other Kv1 channels (Yellen, 1998). However, these agents do not slow inactivation of native g_K (Mathes et al., 1997). Second, we report here that chloramine T (Chl-T) accelerates inactivation of sqKv1A channels and concomitantly leads to irreversible loss of channel activity. Both effects are seen for C-type inactivation with *Shaker* B channels (Schlief et al., 1996). We find that Chl-T affects inactivation of the native channels differently. Third, we find that 4-aminopyridine (4AP) blocks activated sqKv1A channels far better than resting channels, as it does with *Shaker* B channels (see also McCormack et al., 1994). In contrast, 4AP preferentially blocks resting channels in GFL neurons just as it does in giant axons (see also Kirsch et al., 1986). These discrepancies suggest that structural differences exist in the regions surrounding the external and internal mouth of the pore in sqKv1A homotetramers versus native channels.

Use of the *Xenopus* system also facilitated a mutagenesis-based approach to define inactivation of sqKv1A channels. Our results provide no evidence for an N-type mechanism and indicate a conventional C-type process. We also describe the powerful influence of a particular amino acid of the external turret region on inactivation kinetics. This residue (H351) is at the position equivalent to F425 in *Shaker* B, but it's prominent role in C-type inactivation has not been widely recognized (Perez-Cornejo, 1999). Some of these results have appeared in abstract form (Jerng and Gilly, 1999).

MATERIALS AND METHODS

Molecular biology

The plasmid containing sqKv1A cDNA has been previously described (Rosenthal et al., 1996). All experiments described here utilized a version of sqKv1A in which functional expression is enhanced through two mutations in the amino-terminus that do not alter any known functional properties (Liu et al., 2001). Amino acid 5 (Val) was deleted, and Gly-87 was replaced by Arg in the T1 domain. This construct (sqKv1A ΔV5 G87R) is designated as "wild-type" sqKv1A in the present paper. The N-terminal deletion mutant used (sqKv1A Δ1–34 G87R) has been previously described (Liu et al., 2001).

Point mutations were introduced into the sqKv1A ΔV5 G87R construct using the QuikChange site-directed mutagenesis method (Stratagene, La Jolla, CA). Mutations at Ser-375 were confirmed by manual sequencing using a commercial kit based on the dideoxy chain-termination method (Amersham Biotech Inc., Piscataway, NJ). Mutations at His-351 were confirmed by automated sequencing (Applied Biosystems, Foster City, CA). Capped cRNA transcripts were synthesized with the T7 mMessage mMachine in vitro transcription system (Ambion, Austin, TX) after linearizing with *Not*I (New England Biolabs, Beverly, MA).

Oocyte injection and electrophysiology

Stage V and VI oocytes from *Xenopus laevis* (Nasco, Fort Atkinson, WI) were defolliculated by treatment with collagenase (Type IA, Sigma, St. Louis, MO or Type A, Boehringer Mannheim, Indianapolis, IN) according to described protocols (Iverson and Rudy, 1990). cRNA was injected (~0.5–2 ng/oocyte) with a Nanoject microinjector (Drummond, Broomall, PA). Injected oocytes were incubated at 16–18°C in standard ND96 (in mM: 96 NaCl, 2 KCl, 1.8 $CaCl_2$, 1 $MgCl_2$, and 5 HEPES, pH 7.5 with NaOH) supplemented with 5 mM sodium pyruvate and 5 μg/ml gentamycin. Whole-oocyte currents were recorded 1–2 days after injection using a standard two-electrode voltage clamp technique (GeneClamp 500B, Axon Instruments, Foster City, CA). Microelectrodes were filled with 3 M KCl (tip resistances of <1.5–2 MΩ). Currents were filtered at 2 kHz and sampled at ≥1 kHz, depending on the length of depolarization.

The bath solution for two-electrode recordings was either ND96 or a low-chloride version that contained (in mM) 96 sodium gluconate, 2 potassium gluconate, 1.8 $CaCl_2$, 1 $MgSO_4$, and 5 HEPES (pH 7.5). The gluconate salts (and all other reagents) were purchased from Sigma or Aldrich (St. Louis, MO). Chloride replacement was found to greatly improve the stability of sqKv1A currents in two-electrode recordings without altering any properties discussed in this paper. TEA and 4AP replaced sodium on an equimolar basis when these agents were used. To prepare low-chloride TEA-containing solutions, TEA-OH was titrated with gluconic acid.

Cell-attached patch recordings were performed 2–3 days after cRNA injection using a List LM-EPC7 patch clamp (Medical Systems, Greenvale, NY) as previously described (Liu et al., 2001). The bath solution contained (in mM) 140 KCl, 2 $MgCl_2$, 1 $CaCl_2$, 10 HEPES, and 11 mM EGTA (pH 7.3, adjusted with KOH). The pipette solution contained (in mM) 125 NaCl, 15 KCl, 6 $MgCl_2$, 1 $CaCl_2$, and 5 HEPES (pH 7.3, adjusted with NaOH). Patch pipettes were made from Corning glass 7052 (Garner Glass Company, Claremont, CA) and typically had a tip resistance of 1–2 MΩ. Currents were filtered at 2 kHz with an 8-pole Bessel filter (Frequency Devices, Haverhill, MA) and digitized at 1 kHz.

Linear ionic (leak) and capacity currents were subtracted on-line with both recording methods using a conventional P/-4 procedure, except in the case of prepulse protocols designed to assay steady-state inactivation. The latter measurements were carried out with the two-electrode method only when the leak current was <100–150 nA at the holding potential of −60 or −70 mV. Temperature was 22–24°C for all experiments.

Electrophysiology with squid GFL neurons

Neurons were manually dissociated from the GFL portion of the stellate ganglion of adult *Loligo opalescens* collected locally and maintained as previously described (Gilly et al., 1990) with minor modifications. GFL neurons were plated onto 5-mm glass coverslips (Bellco Glass, Inc., Vineland, NJ) that had been coated with 2% concanavilin A in a manner similar to that originally described. In addition, 5 mM trehalose was added to the culture medium, pH was increased to 8.0, and incubation temperature was lowered to 12–14°C. Neurons were normally used within 5–6 days of plating. Properties of K^+ currents (I_K) described in this report do not appear to change over this time, although density of I_K increases somewhat (unpublished data).

Whole-cell recordings were carried out as previously described (Mathes et al., 1997). The external solution contained (in mM) 470 NaCl, 10 KCl, 10 $CaCl_2$, 20 $MgCl_2$, 20 $MgSO_4$, 0.2 tetrodotoxin, 10 HEPES (pH 7.8–8.0). NaCl was replaced with KCl on an equimolar basis for those experiments with high external K^+. The internal solution contained (in mM) 20 KCl, 50 KF, 80 potassium glutamate, 10 lysine (titrated to pH 7 with HEPES), 1 EGTA, 1 EDTA, 381 glycine, 291 sucrose, 4 MgATP. Final pH was set to 7.8 with tetramethylammonium hydroxide.

Recordings were carried out at 20–24°C. Holding potential was −80 mV unless otherwise noted. P/-4 subtraction was carried out on-line as described above. Signals were generally sampled at either 20 kHz (or 1 kHz) and filtered at 6 kHz (or at 2 kHz) with an 8-pole Bessel filter (LPF-8, Warner Inst., Hamden, CT).

Data acquisition and analysis

Data acquisition and pulse generation used desktop personal computers and either a custom-built interface and software (D. R. Matteson, Dept. of Physiology, University of Maryland) or a commercial package (Digidata 1200A interface and pClamp 7.0; Axon Instruments). Additional data analysis used Sigmaplot (Jandel, San Rafael, CA) and Igor Pro (Wavemetrics, Eugene OR). Results are expressed as means ± SD.

RESULTS

Activation and inactivation of sqKv1A channels in oocytes

Outward K^+ currents (I_K) recorded in a cell-attached patch from an oocyte expressing sqKv1A channels activate rapidly and inactivate incompletely to a steady-state level in ~500 ms at room temperature (Fig. 1 *A*). The time course of I_K decay due to inactivation is well described by a single exponential with a time constant of ~120 ms at all voltages

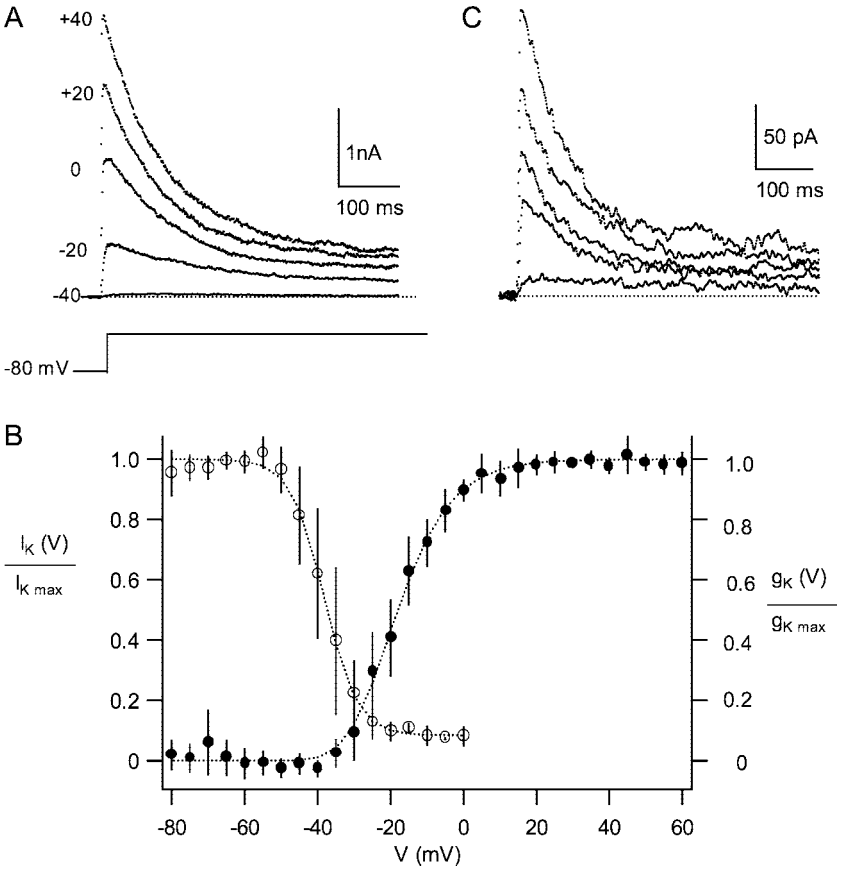

FIGURE 1 Voltage-dependent properties of sqKv1A channels and genetic truncation of the N-terminus. (*A*) Macroscopic I_K to the indicated voltages in a cell-attached patch. (*B*) Voltage-dependence of steady-state inactivation (○) and peak g_K (●) determined as described in the text. Data are means ± SD ($n = 5$). Solid curves represent fits using a first-power (for inactivation) or a fourth-power (for g_K) Boltzmann function (see legend to Table 1). (*C*) Macroscopic I_K of the N-terminal deletion mutant, sqKv1A Δ1–34. Voltages are the same as in *A*.

from +10 to +60 mV (fits not illustrated). This value is about twice that observed at 18°C for sqKv1A channels expressed in *Sf*9 cells (Brock et al., 2001), but the reasons for this difference are not clear. In neither case do sqKv1A channels display a biphasic inactivation time course like that shown by their proposed native counterparts in GFL neurons or giant axons (Mathes et al., 1997).

The relationship between voltage-dependent activation and steady-state inactivation for sqKv1A channels in oocytes is illustrated in Fig. 1 *B*. Conductance (g_K) at a given voltage (V) was determined from the change in I_K amplitude (ΔI_K) following repolarization at the time of peak I_K to the holding potential (V_H) as $g_K = \Delta I_K/(V - V_H)$. Values of $g_K(V)$ thus determined were normalized by maximal g_K (g_{Kmax}), and the normalized g_K-V curve (●, Fig. 1 *B*) is well fit by a fourth-power Boltzmann function with a voltage midpoint (V_a) of −34 mV and a steepness parameter (s_a) of 9 mV/e-fold change. These fits are useful for comparing wild-type and mutant channels and are not intended to support a specific model of activation (see below and legend to Table 1).

Steady-state inactivation was determined by assaying the amplitude of I_K at +60 mV following a prepulse of 10 s duration to voltages between −80 mV and 0 mV and normalizing to maximal I_K, I_{Kmax} (○, Fig. 1 *B*). This relationship is adequately described by a first-power Boltzmann distribution with a midpoint voltage (V_i) of −35 mV and steepness (s_i) of 4 mV/e-fold change. Similar results were obtained from two-electrode recordings (see Table 1).

SqKv1A channels do not inactivate by an N-type mechanism

To test the possibility that the N-terminus might contribute to sqKv1A inactivation (Hoshi et al., 1990), a genetic truncation mutant was created (sqKv1A Δ1–34 G87R) starting at the naturally occurring Met-35 residue of sqKv1A. This eliminates the N-terminus almost to the beginning of the T1 domain. Inactivation of these mutant channels is essentially unchanged (Fig. 1 *C*), suggesting that inactivation does not involve a conventional N-terminal element.

This finding is also consistent with the fact that inactivation properties of sqKv1A channels are virtually identical to those observed for the naturally occurring splice variants sqKv1B and sqKv1D when expressed in oocytes (Rosenthal et al., 1997; Liu et al., 2001). These variants possess truncated N-termini with respect to sqKv1A (13 and 34 amino acids, respectively) and have several amino acid differences in the T1 domain and C-terminus, but they show identical primary structures from S1 through S6.

In addition, the effect of internal TEA on inactivation was tested for sqKv1A channels. I_K was recorded using a two-

TABLE 1 Parameters of macroscopic activation and inactivation

	Wild Type	S375V	S375T	H351F	H351G	H351A	H351D	H351K
V_a^* (mV)	−35 ± 1	−38 ± 2	−33 ± 2	−35 ± 1	−42 ± 1	−34 ± 2	−36 ± 2	−38 ± 3
s_a (mV/*e*-fold)	11.5 ± 0.5	20.3 ± 1.2	15.0 ± 2.8	10.0 ± 1.1	16.3 ± 1.0	16.3 ± 1.7	17.5 ± 2.4	18.4 ± 2.7
(*n*)	(5)	(3)	(3)	(4)	(3)	(3)	(3)	(3)
$V_i^\dagger$ (mV)	−35 ± 1	−34 ± 1	−33 ± 1	−35 ± 1	−37 ± 1	−30 ± 1	−27 ± 1	−31 ± 2
s_i (mV/*e*-fold)	4.5 ± 0.4	5.2 ± 1.1	4.6 ± 0.8	4.2 ± 0.3	4.8 ± 0.5	5.0 ± 0.7	5.9 ± 0.6	4.5 ± 0.5
c_i	0.13 ± 0.00	0.11 ± 0.03	0.11 ± 0.01	0.18 ± 0.06	0.14 ± 0.03	0.12 ± 0.03	0.13 ± 0.02	0.13 ± 0.00
(*n*)	(4)	(3)	(4)	(3)	(3)	(4)	(4)	(3)
$\tau_{inact}^\ddagger$ (ms)	251 ± 15	4236 ± 1373	4091 ± 547	172 ± 9	135 ± 7	2767	3281 ± 209	3346 ± 165
A_s	0.18 ± 0.01	0.15 ± 0.03	0.16 ± 0.04	0.19 ± 0.03	0.29 ± 0.03	0.19	0.20 ± 0.04	0.18 ± 0.01
(*n*)	(6)	(3)	(3)	(3)	(8)	(1)	(3)	(3)

*Values corresponding to the activation parameters obtained from the g_K-V curve as described in the text. These data were fit with a fourth-order Boltzmann distribution. $g_K = g_{Kmax}/[1 + \exp(V_a - V)/s_a]^4$, where g_{Kmax} is maximum peak g_K, V_a is the midpoint voltage for activation of one subunit, and s_a is the slope factor. All values in this table are presented as means ± SD from n independent determinations (n).

†Values corresponding to the inactivation parameters obtained from prepulse experiments (see text). I_K-V curves were well described assuming a simple Boltzmann distribution. $I_K = I_{Kmax}/[1 + \exp(V - V_i)/s_i] + c_i$, where I_{Kmax} is maximum peak I_K, V_i is the midpoint voltage of the distribution, V is prepulse voltage, s_i is the slope factor, and c_i is the steady-state fraction.

‡τ_{inact} is the time constant of inactivation at +60 mV. A_s is the fractional amplitude of steady-state I_K.

electrode voltage clamp from several oocytes before and after injecting TEA-Cl to achieve a final internal concentration of 5 mM (calculated assuming an oocyte diameter of 1 mm). TEA injection reduced I_K by ~75% but did not alter time course of inactivation (data not shown), as would be expected for a conventional N-type mechanism (Choi et al., 1991). This finding, along with the genetic evidence discussed above, makes it unlikely that inactivation of sqKv1A channels involves a conventional N-type mechanism.

Effects of external TEA and K^+ ions on inactivation kinetics

TEA and K^+ ions interact with the external mouth of Kv1 channels by either blocking or permeating, respectively. Transient block of the conducting pore by TEA prevents entry of the channel into the C-inactivated state, and this competition between TEA and inactivation results in slowing of inactivation kinetics (Grissmer and Cahalan, 1989; Choi et al., 1991). K^+ ions similarly slow C-type inactivation by stabilizing the open state (Yellen, 1998).

External TEA and K^+ ions were tested on sqKv1A channels expressed in oocytes using the two-electrode voltage-clamp. In agreement with data from *Sf*9 cells (Brock et al., 2001), TEA slowed the rate of inactivation by approximately the same degree as that observed for I_K amplitude reduction (Fig. 2, *A* and *B*). Elevated concentrations of external K^+ also dramatically slowed inactivation of sqKv1A channels in oocytes (Fig. 2 *C*). Inactivation on a longer time scale was monitored by periodically sampling I_K during 5-s pulses to +60 mV in the presence of external K^+ concentrations of 2–98 mM. Data in Fig. 2 *D* reveal a slowing of 7.6-fold over this range. In addition, the fraction of non-inactivating I_K also increases with increasing external K^+. This latter effect is also seen for native g_K (Mathes et al., 1997).

C-type inactivation of sqKv1A is supported by mutagenesis studies

A mutagenesis approach was also used to test whether a C-type inactivation mechanism is a property of sqKv1A channels. Point mutations of the sqKv1A α-subunit were introduced at the residue (Ser-375) corresponding to Thr-449 in *Shaker* B, an amino acid critical to C-type inactivation (Lopez-Barneo et al., 1993). Families of I_K records from cell-attached patches are illustrated in Fig. 3 for wild-type SqKv1A (Fig. 3 *A*) and for substitutions of Ser-375 by Thr (S375T, Fig. 3 *B*) and by Val (S375V, Fig. 3 *C*). Both substitutions dramatically slow inactivation, and the time course of I_K at +60 mV is compared for wild-type, S375T, and S375V channels in Fig. 3 *D*. Similar results were obtained with two-electrode recordings. As indicated in Table 1, these effects on inactivation kinetics are accompanied by only small changes in activation and steady-state inactivation parameters (see Table 1).

These results are similar to those reported for the same amino acids at position 449 of *Shaker* B. C-type inactivation is very fast with Ser at position 449 (Schlief et al., 1996), Val-449 produces the slowest inactivation (Lopez-Barneo et al., 1993), and the *Shaker* B wild-type Thr-449 is intermediate. Thus, in agreement with the pharmacological findings discussed above, our mutational analysis supports a C-type inactivation mechanism for sqKv1A channels that is fundamentally similar to that in *Shaker* B.

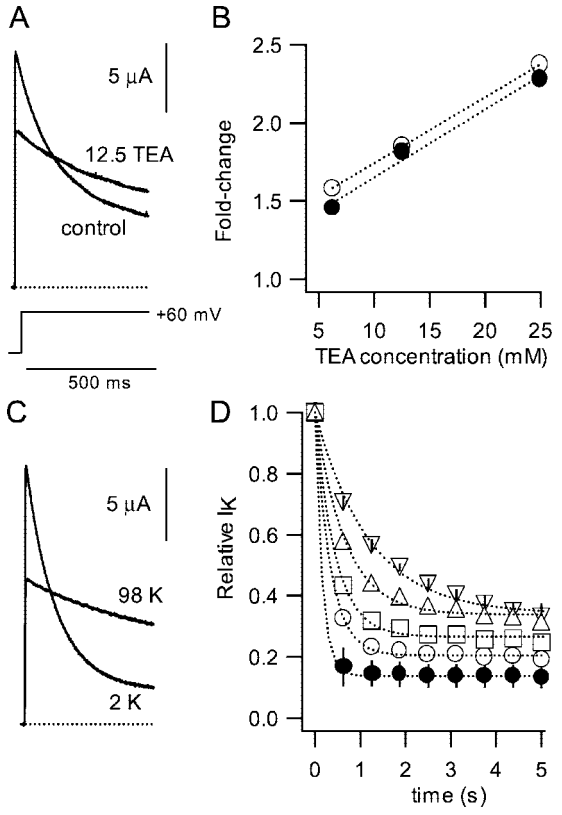

FIGURE 2 Effects of external TEA and external K^+ on sqKv1A channels. (*A*) I_K traces are illustrated at +60 mV with and without 12.5 mM TEA in the bath solution. (*B*) Block of I_K (○) and slowing of inactivation (●) depend similarly on TEA concentration. Degree of block by TEA was assessed by comparing peak I_K before and after TEA application (fold-change = I_K (control)/I_K (TEA)). The time course of inactivation in all cases was well fit by a single exponential (τ), and fold-change in kinetics is defined as τ (TEA)/τ (control). The straight line represents a linear regression. (*C*) Effects of elevated external K^+ on the time course of inactivation. I_K traces at +40 mV with either 2 or 98 mM external K^+ are illustrated. (*D*) To observe effects on inactivation over a longer time scale, I_K at +60 mV was sampled until it reached its peak value and was then periodically sampled for several ms over 5 s, as indicated by the individual symbols. Data are plotted as means from several experiments at the following K^+ concentrations, and single exponential fits (τ) are illustrated: 2 mM (●; τ = 157 ms), 14 mM (○; τ = 336 ms), 26 mM (□; τ = 442 ms), 50 mM (△; τ = 662 ms), and 98 mM K^+ (▽; τ = 1196 ms). Standard deviations are available only for 2 mM and 98 mM data.

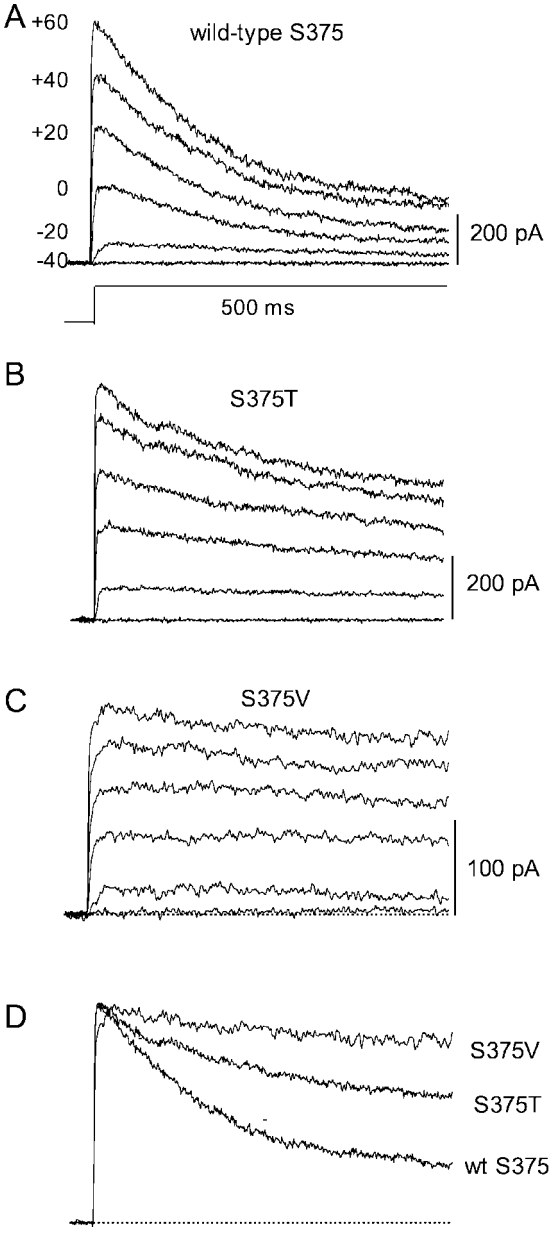

FIGURE 3 Alterations of inactivation time course by amino acid substitutions of serine 375, a position that corresponds to T449 in *Shaker* B channels. Families of I_K traces at the indicated voltages are illustrated for wild-type sqKv1A (*A*), S375T (*B*), and S375V (*C*) channels. (*D*) Normalized traces at +60 mV from panels *A*–*C* are superimposed.

Residue 351 of the sqKv1A α-subunit is also critical to C-type inactivation

Titration of a histidine residue (His-351) underlies the pH-sensitivity of block of sqKv1A channels by tityustoxin-Kα (Ellis et al., 2001). This residue corresponds to Phe-425 of *Shaker* B, and substitution of His at this site (F425H) leads to pH-dependent charybdotoxin binding and increases the pH-sensitivity of C-type inactivation (Perez-Cornejo et al., 1998; Perez-Cornejo, 1999; Thompson and Begenisich, 2000). Because the turret and P-region of *Shaker* B and sqKv1A are highly conserved, we created a series of amino acid substitutions for His-351 to test the importance of this position to C-type inactivation.

Fig. 4 *A* presents results for the indicated mutants; in each case, I_K at +60 mV is illustrated (two-electrode recordings). It is clear that the nature of the amino acid at position 351 has a profound influence on the rate of inactivation (see Table 1). Bulky, hydrophobic residues (H351W and H351F) lead to faster inactivation in comparison to the wild-type channels. Glycine (H351G), a small, polar residue, displays a rate similar

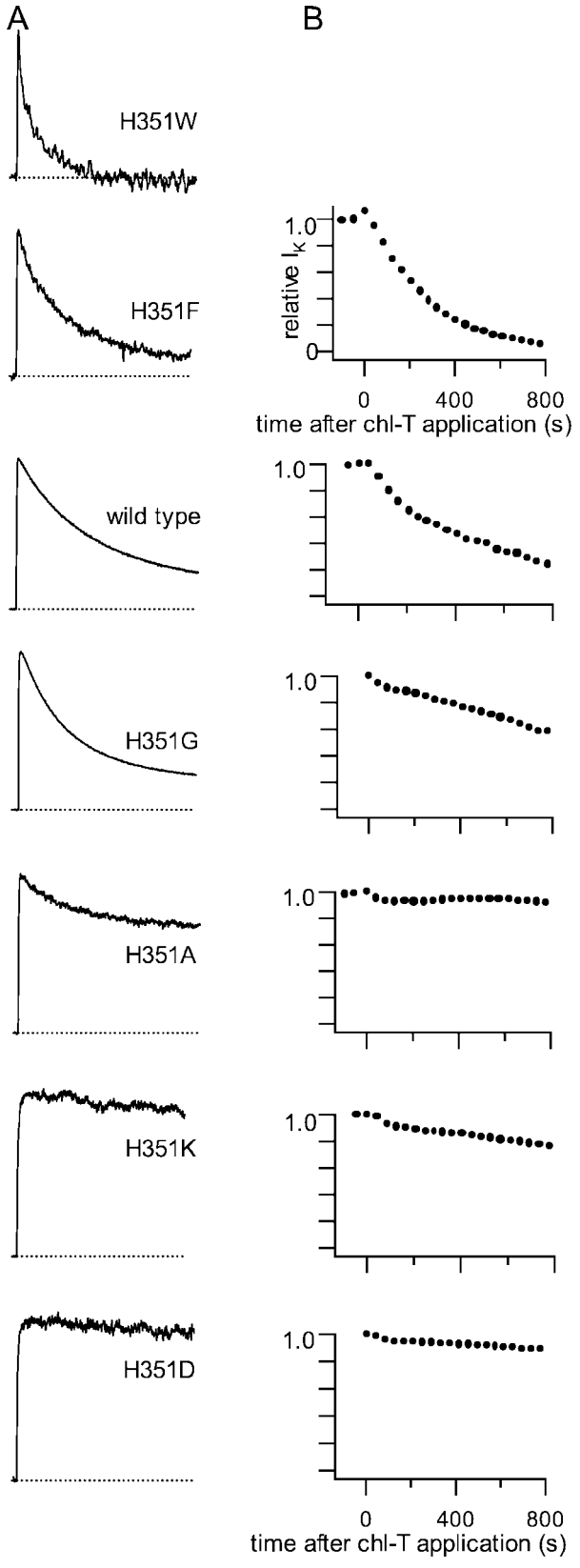

FIGURE 4 Inactivation of channels with amino acid substitutions at position 351 and associated run-down induced by Chl-T treatment. (*A*) Representative I_K traces at +60 mV for wild-type (H351) and the series of mutant channels as indicated. Amplitudes have been normalized. The H351W and H351F mutations brought about severely and moderately decreased expression, respectively. I_K traces for H351W, H351F, wild-type, and H351G are from two-electrode voltage clamp. I_K for H351A, H351K, and H351D are from cell-attached patches, but corresponding records with two-electrode voltage clamp are nearly identical (not illustrated). (*B*) Time course of I_K rundown in the presence of 250 μM Chl-T for the series of H351 mutations. Data are not available (NA) for H351W because of poor expression. Protocol used was identical to that described in conjunction with Fig. 5 *A*.

to wild-type channels, but substitution by nonpolar alanine (H351A) leads to a marked slowing (Table 1). Charged residues, both acidic (H351D) and basic (H351K) also greatly slow inactivation. No functional expression was obtained with H351N and H351C (not illustrated). Data in Table 1 indicate that none of the H351 substitutions have large effects on activation, suggesting that the amino acid at this position is directly influencing the inactivation process.

Sensitivity of wild-type sqKv1A channels and of H351 mutants to oxidation by chloramine-T: a link to C-type inactivation

Studies of *Shaker* B channels lacking N-type inactivation show that treatment by the oxidant chloramine T (Chl-T) leads to a progressive and irreversible reduction of peak I_K ("rundown") with a time course that is positively correlated to Chl-T concentration and to the rate of C-type inactivation (Schlief et al., 1996). Differential sensitivity to Chl-T treatment of the H351 mutants was therefore tested as a means of associating the functional changes observed for these mutations with modification of a C-type inactivation mechanism.

I_K from oocytes expressing wild-type sqKv1A channels exhibits rundown following Chl-T application, as monitored by delivering 700-ms pulses to +60 mV every 41 s, an interval sufficiently long to allow complete recovery from inactivation (Fig. 5 *A*). The time course was analyzed by normalizing peak I_K at each time, $I_K(t)$, to the last pulse before Chl-T application, $I_K(0)$. Examples of data and single-exponential fits for several Chl-T concentrations are shown in Fig. 5 *B*. Time constants for 250 μM (●), 500 μM (○), and 1 mM Chl-T (□) were respectively 462 ± 109 s (n = 3), 295 ± 57 s (n = 3), and 192 ± 16 s (n = 3). At a concentration of 50 μM (△) Chl-T decreased peak I_K only by ~10% after 13 min, and this concentration thus represents an approximate "threshold" for a detectable effect.

This experiment was also carried out with the H351 mutants using 250 μM Chl-T (Fig. 4 *B*). For H351F, the slightly faster inactivation (relative to wild-type) was associated with faster I_K rundown. Conversely, rundown was much slower in those mutants with slowed inactivation (H351A, H351D, and H351K). Glycine appears to be an exception, because rundown is slower than that of wild-type, even though inactivation is fairly normal. A similar correlation between the kinetics of Chl-T-induced rundown

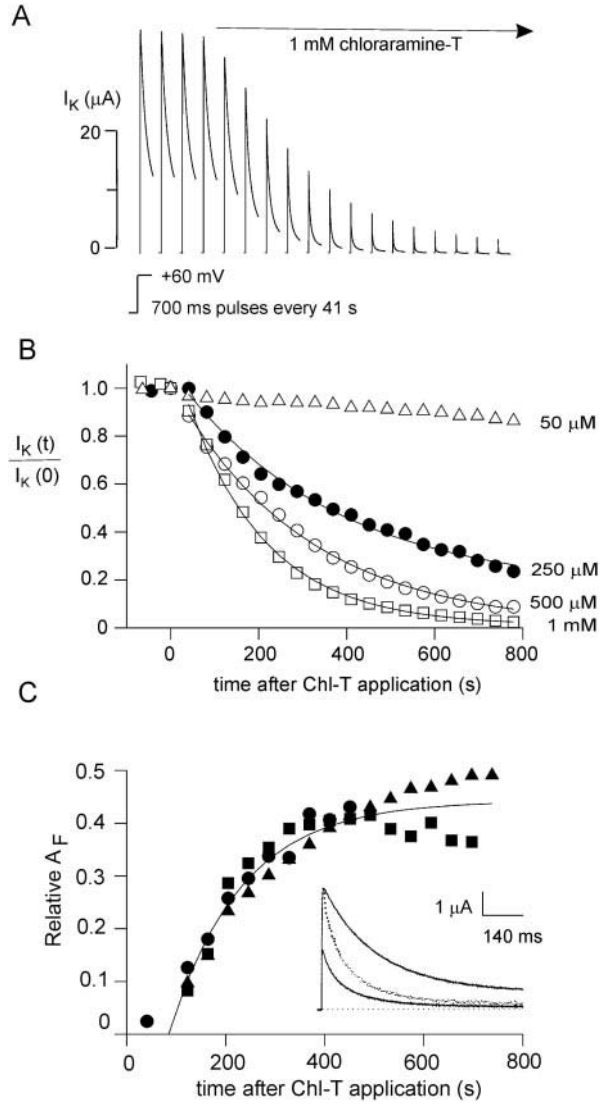

FIGURE 5 I_K rundown and modification of sqKv1A inactivation by Chl-T. (*A*) Effect of Chl-T treatment on I_K amplitude and kinetics. Pulses of 700-ms duration to +60 mV were applied every 41 s in the absence and presence of externally applied Chl-T. Inter-pulse periods are not plotted on a true time scale. (*B*) Concentration dependence of Chl-T induced rundown. Time course of rundown is displayed as the decline in peak I_K over time for 50 μM (△), 250 μM (●), 500 μM (○), and 1 mM Chl-T (□). I_K rundown at Chl-T concentrations ≥250 μM) was well described by a single exponential. (*C*) Rundown is accompanied by an acceleration of inactivation. *Inset:* Solid traces represent I_K before treatment with 250 μM Chl-T and midway during the rundown process. The dotted trace represents the after-rundown trace scaled to match the pretreatment peak I_K. *Main figure:* Quantitative description of the inactivation of sqKv1A channels after Chl-T treatment required fitting with two exponentials, which reveals the appearance and progressive increase in the fractional amplitude of the rapidly inactivating component (A_F). Data from the fittings of three experiments are plotted, and the solid trace illustrates the best exponential fit. See text for additional details.

and inactivation was described for C-type inactivation in *Shaker* B (Schlief et al., 1996). Our results thus support the idea that the amino acid at position 351 plays an important role in C-type inactivation of sqKv1A channels.

Differential effects of Chl-T treatment on inactivation of sqKv1A and native K^+ channels

Studies on *Shaker* B channels have also indicated that the rate of C-type inactivation is accelerated by application of Chl-T, and this effect is manifested by the appearance of a rapidly inactivating component ($\tau \sim 25$ ms; Schlief et al., 1996). Inactivation of sqKv1A channels was also accelerated following Chl-T application, as indicated by comparison of I_K traces recorded before application and midway during the rundown period (Fig. 5 *C*, *inset*; dotted trace has been scaled). Before application of Chl-T, the time course of I_K decay is well fit by a single exponential with a time constant of ~150 ms, but after treatment, a biexponential fit was necessary with half of the fractional amplitude in a rapidly inactivating component. This analysis, carried out on four separate experiments, yielded the following parameters (means ± SD): fast component fractional amplitude (A_F) = 0.45 ± 0.02 and time constant (τ_F) = 38 ± 4 ms; slow component amplitude (A_S) = 0.45 ± 0.02 and time constant (τ_S) = 150 ± 15 ms; non-inactivating fractional amplitude (A_{NI}) = 0.04 ± 0.02.

Development of the rapidly inactivating component during Chl-T treatment does not occur with the same time course as I_K rundown (compare Fig. 5, *B* and *C*). The time course of the increase in A_F in 250 μM Chl-T is well described with a single exponential with a time constant of ~146 s (Fig. 5 *C*, *solid curve*), whereas rundown at this concentration is about three times slower (see above). This suggests that the loss of I_K and the appearance of the rapidly inactivating component are not due to a single Chl-T-induced modification.

Experiments similar to those described above were also carried out with GFL neurons. Although Chl-T induces I_K rundown in a way similar to that described above for sqKv1A, the time course of inactivation in GFL neurons is not accelerated. Fig. 6 *A* shows the effect of 125 μM Chl-T on peak I_K amplitude (○; 500 ms pulses to +40 mV) normalized to the last measurement before Chl-T application (time 0). The time course of I_K rundown can be described by a single exponential with a time constant of 490 s (*open symbols*; fit not shown), a value comparable to that observed for 250 μM Chl-T acting on sqKv1A.

Data are also shown in Fig. 6 *A* for another experiment in which Chl-T was sequentially applied at increasing concentrations of 5, 10, and 50 μM; 50 μM Chl-T induces a detectable rundown of I_K that progresses with an estimated time constant of ~1900 s (fit not illustrated), and this "threshold" concentration is thus similar to that observed for sqKv1A.

Despite this similarity in the effect of Chl-T on native and cloned squid channels, Chl-T treatment altered the time course of inactivation of native I_K in a manner essentially opposite to that described above for sqKv1A and *Shaker* B. Fig. 6 *B* shows I_K obtained before application of 125 μM

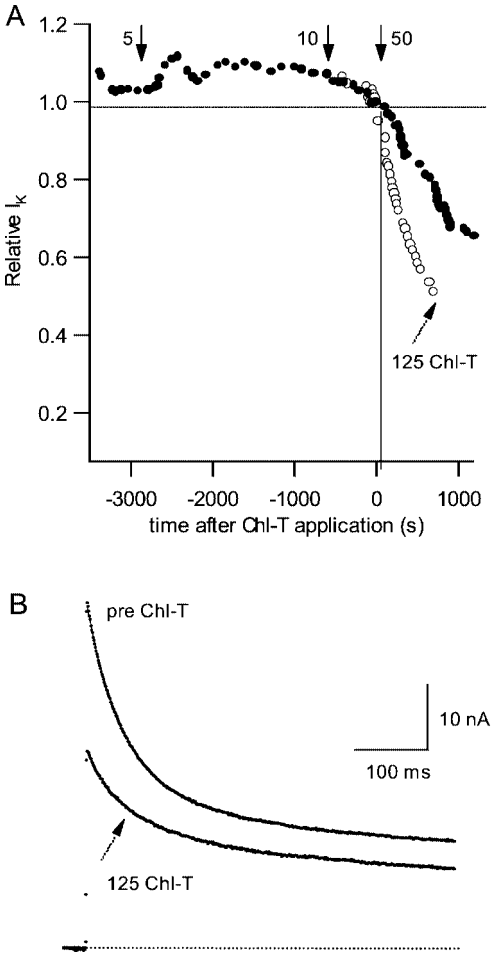

FIGURE 6 Chloramine T effects on native g_K of GFL neurons. (*A*) Time course of the change in peak I_K following application of Chl-T. Results from two experiments are shown. In one, 125 μM Chl-T (○) was applied at time 0. In the other (●), sequential applications of 5, 10, and 50 μM Chl-T were performed at the times indicated by arrows. (*B*) Change in the I_K inactivation time course produced over 9 min in the presence of 125 μM Chl-T. Fitting of rapidly and slowly inactivating I_K components are described in detail in the text, and the corresponding fits are superimposed on the illustrated traces. See text for fitting details.

Chl-T. Under the recording conditions used here (+40 mV; 22°C) the majority of inactivation is fast (Mathes et al., 1997), and a double-exponential fit of the pre Chl-T trace is illustrated (fast A_F = 25.5 nA and τ_F = 43.3 ms; slow A_S = 12.1 nA and τ_S = 218 ms; non-inactivating A_{NI} = 15.1 nA). Following Chl-T treatment, the illustrated fit corresponds to a reduction of A_F by a factor of 0.36 with much smaller amplitude reductions for the slowly and non-inactivating fractions (0.82 and 0.72, respectively). Neither fast nor slow time constants were significantly changed, however (41.9 ms and 240 ms, respectively). Similar results were obtained in several other experiments, although in some cases all components were reduced more equally. At any rate, the rapidly inactivating component of native I_K is clearly decreased by Chl-T, unlike the results with sqKv1A channels. In both cases, sensitivity of inactivation kinetics to external TEA or K^+ is not qualitatively altered by Chl-T treatment (data not illustrated).

Comparison of the actions of 4AP on native K^+ channels and sqKv1A expressed in oocytes

Characterization of 4AP block of voltage-gated K^+ channels was originally carried out on squid giant axons, where it was found that channels were blocked at typical negative holding potentials and depolarizing voltage steps resulted in a time- and voltage-dependent relief of block (Yeh et al., 1976; Kirsch et al., 1986). Block could be restored by prolonged repolarization to negative potentials. These authors concluded that 4AP binds to the K^+ channels in a resting, closed state that was at an intermediate position in the activation pathway and thereby hinders activation from progressing beyond this state toward channel opening.

These early studies were hampered by the inability to utilize long voltage-clamp steps with the axial-wire voltage-clamp method, and therefore many of the measurements were not straightforward. We have reexamined the actions of 4AP on the same native channels in GFL neurons using whole-cell voltage-clamp, and these results can thus be more directly compared with those on cloned channels expressed in oocytes.

Fig. 7 *A* confirms that a low concentration of 4AP (0.1 mM) blocks most of the native GFL K^+ channels at −100 mV in the absence of any activating pulses. The first trace in 4AP was recorded 7 min after changing solutions with the cell continuously held at −100 mV (no intervening pulses). Three additional traces taken at 1-min intervals are also illustrated. The small additional decrease was typical, but this effect was not explored in detail.

SqKv1A channels in oocytes display basically the opposite state-dependency for 4AP-block. Thus, resting channels are insensitive and activation enhances block. Application of 0.1 mM 4AP to non-inactivating S375V channels at −80 mV for 7 min with no intervening pulses did not affect peak I_K at 0 mV (fraction blocked = 0.04 ± 0.07, n = 4). At much higher 4AP concentrations (5–10 mM) block of resting sqKv1A channels did occur (see also below).

Activation of sqKv1A channels markedly enhances the ability of 4AP to block. Exposure of non-inactivating sqKv1A S375V channels to 0.5 mM 4AP at −80 mV for >2 min produced no decrease in peak I_K for the first test pulse to −20 mV (Fig. 7 *C*; compare *control* and *trace 1*). I_K appears to inactivate, but this reflects time-dependent block of activated channels by 4AP. After three more pulses at 2-min intervals, a steady level of block is attained (fractional block of peak I_K = 0.59 ± 0.03, n = 3). Similar results were obtained with wild-type sqKv1A channels.

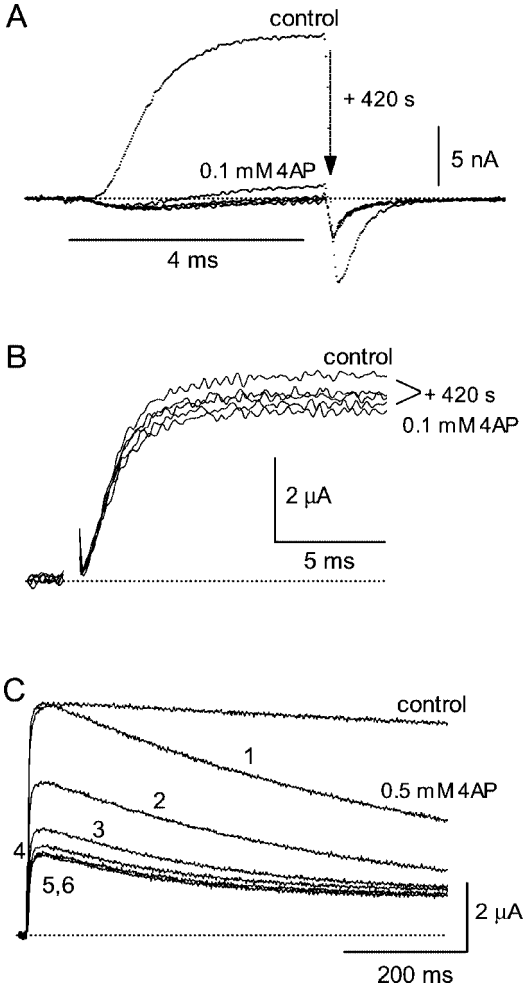

FIGURE 7 Effects of 4AP on native g_K of GFL neurons and on sqKv1A in oocytes. (*A*) Block of resting GFL channels tested at +40 mV from a holding potential of −100 mV. The arrow points to the first trace recorded after applying 0.1 mM 4AP for 7 min. Three additional illustrated traces in 4AP were recorded subsequently as described in the text. The small inward current that persists in the presence of 4AP is due to calcium channels; this amount of I_{Ca} is typical (McFarlane and Gilly; 1996. (*B*) I_K (+40 mV) was recorded from an oocyte expressing non-inactivating sqKv1A S375V channels in the same manner as described for *A*. Virtually no resting block is evident. (*C*) Activation enhances block of sqKv1A S375V channels by 0.5 mM 4AP. I_K (+40 mV) declines during the first long pulse (1) delivered after exposure to 4AP. Subsequent pulses (2–4) show an incremental degree of block until a steady level of block is achieved by pulses 5 and 6.

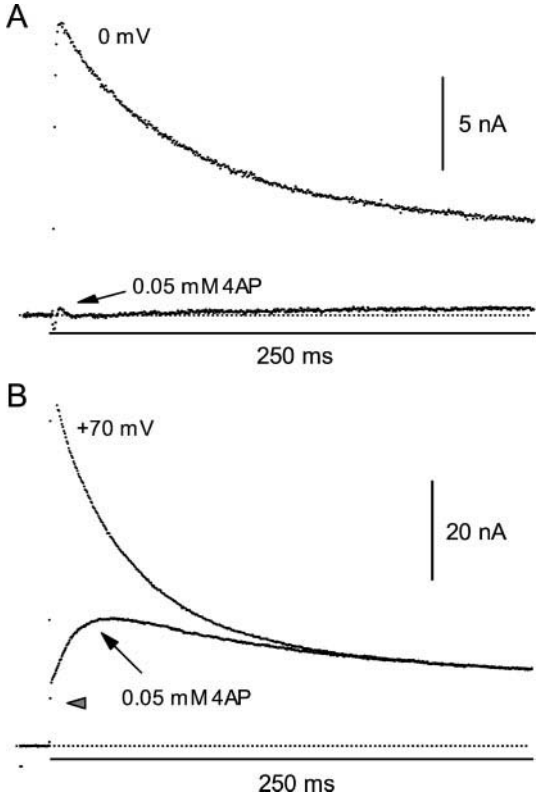

FIGURE 8 Voltage-dependent relief of 4AP block from activated native channels in a GFL neuron. (*A*) Block of peak I_K (0 mV) by 0.05 mM 4AP is indicated by the arrow. Little sign of relief is evident during the pulse. (*B*) Approximate block of peak I_K at +70 mV is indicated by the arrowhead. Rapid relief of 4AP block results in an increase in I_K that peaks and then inactivates.

Relief of 4AP block produced by activation

Voltage- and time-dependent relief from 4AP block is demonstrated in Fig. 8 for native GFL K^+ channels. At 0 mV (Fig. 8 *A*) 0.05 mM 4AP blocks most I_K, and there is little sign of relief during the pulse. However, at +70 mV (Fig. 8 *B*) there is a marked rise in I_K from an initial level that reflects channels that were not blocked at the start of the pulse. This level is difficult to define unambiguously, because relief is so fast, but it lies somewhere below the left-pointing arrowhead. Channels that are relieved from block can apparently inactivate, and the overall I_K time course is thus dictated by both the rates of relief of block and of inactivation. Relief of 4AP block with sqKv1A channels is much slower and less pronounced, only becoming apparent at very positive voltages, i.e., above >+80 mV (not illustrated). This phenomenon was not studied in detail.

Reestablishment of 4AP block of native channels following activation-dependent relief

Fig. 9 *A* shows the slow activation due to relief of block by 0.01 mM 4AP and subsequent inactivation of native I_K in a GFL neuron at +40 mV as described in conjunction with Fig. 8. The first 30 ms of another pulse in 4AP is illustrated on an expanded time base in Fig. 9 *B* (*pulse 1*), and steady-state I_K at 750 ms is indicated (Δ). After repolarization to −80 mV for 2 s, a second pulse to +40 mV resulted in a rapidly activating I_K (*pulse 2*, right half of Fig. 9 *B*) that is nearly as large as the pre-4AP control (Fig. 9 *A*).

This phenomenon was seen in every GFL neuron thus studied and is similar to the pattern reported for native channels underlying I_{to} in mammalian heart (Campbell et

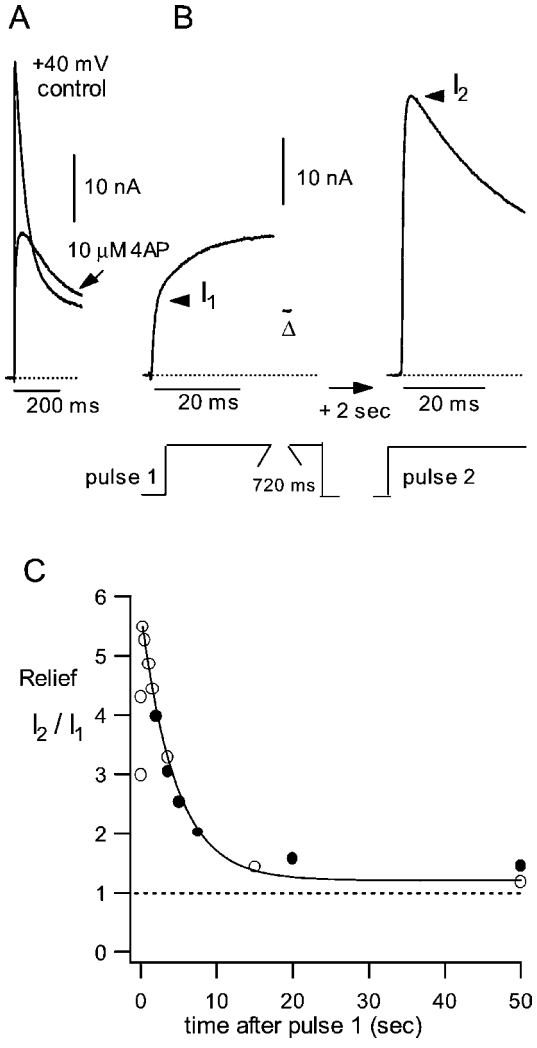

FIGURE 9 Restoration of 4AP-block of resting native channels in GFL neurons following relief of block due to a strong depolarization. (*A*) Relief of block as described in conjunction with Fig. 8 *B* is evident during a 250-ms pulse to +40 mV. (*B*) Left panel shows I_K during the initial 30 ms of a 750-ms pulse to +40 mV in the presence of 10 μM 4AP from the same experiment as in *A*. I_1 indicates the approximate level of I_K due to unblocked channels at the start of pulse 1; the slower rise is due to relief of block. The final I_K level at 750 ms is indicated (Δ). Following repolarization to −80 mV for 2 s, a 30-ms pulse to +40 mV produced I_K as illustrated in the right-hand panel (pulse 2). Peak I_K (I_2) is much larger than I_1 because many channels have been relieved of 4AP-block during the preceding long pulse. See text for additional details. (*C*) Time course of restoration of resting-channel block. The inter-pulse interval as described above was varied, and the ratio I_2/I_1, an index of the amount of block relief, is plotted versus inter-pulse interval. These data are fit well by a single time constant of ~4 s (*solid curve*). Filled symbols are for 40 mM external K^+; open symbols are for 500 mM external K^+.

al., 1993). The "extra" peak I_K in pulse 2 appears to represent channels that have become unblocked during pulse 1, which then inactivate. Following repolarization, these channels become available to contribute to I_K as they recover from inactivation—provided pulse 2 is delivered before recovered channels can be blocked again by 4AP at the resting potential. Thus, by varying the interval between pulses 1 and 2, an estimate of the time course of resting-channel block can be obtained. Results using this approach from two cells in 40 mm external K^+ (●) and in 500 (○) mM K^+ are illustrated in Fig. 9 *C*, and a time constant of ~4 s is evident. High external K^+ does not appreciably affect the rate of block of resting native channels.

Only a few experiments of this type were carried out on oocytes expressing wild-type sqKv1A channels, but there was no sign of reestablishment of resting block at −70 mV in the presence of 4AP concentrations as high as 1 mM for inter-pulse intervals of 200 s (not illustrated). This is consistent with poor block of resting sqKv1A channels as discussed above.

Comparison of 4AP-affinity for native and sqKv1A channels

To compare the affinities of sqKv1A and native channels for 4AP at the holding potential we carried out dose-response analysis for both, and results are illustrated in Fig. 10. Measurements of peak I_K for native channels (Fig. 10 *A*) used brief pulses (5 ms) to 0 mV to minimize relief of block after maximal block was established, as described for Fig. 7 *A*. This gives an estimate of the affinity for the resting channels. The 4AP-affinity of resting sqKv1A channels was carried out using similar test pulses, but these were the first pulses after applying a given concentration of 4AP and waiting 5–7 min (Fig. 10 *B*). To measure 4AP affinity of activated sqKv1A channels, test pulses were preceded by four to five long pulses (750 ms) to −10 mV to maximize the fraction of channels blocked at the holding potential. Test pulses were delivered 10–20 s after the final "conditioning" pulse (Fig. 10 *C*).

Hill-plot analysis (Fig. 10 *D*) yields K_d values of 5 μM for resting native channels, 3.2 mM for resting sqKv1A, and 75 μM for activated sqKv1A. Although waiting for a longer period before the first pulse would reduce the apparent K_d for resting sqKv1A channels, it is unlikely that the large difference for resting native versus sqKv1A channels would be drastically affected.

DISCUSSION

In this paper we positively identify the inactivation mechanism of sqKv1A channels as being C-type with both mutagenesis and pharmacological tests using TEA, K^+, and Chl-T. All of these agents interact with C-type inactivation in *Shaker* B channels in characteristic ways that are clearly evident with sqKv1A channels. Results in this paper add to and greatly expand previous studies (Mathes et al., 1997; Brock et al., 2001) in demonstrating significant disparities in the actions of each of these pharmacological agents for

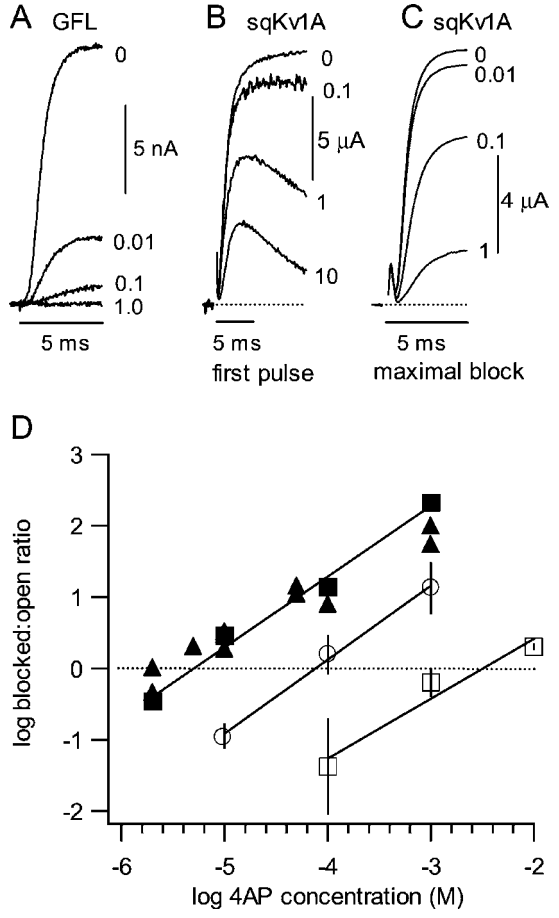

FIGURE 10 Dose-response analysis of 4AP-block for native g_K of GFL neurons and sqKv1A expressed in oocytes. (*A*) Representative I_K traces from an experiment with a GFL neuron are illustrated. Labeled 4AP concentrations are in mM. Small non-inactivating calcium currents (McFarlane and Gilly, 1996) were removed from the illustrated I_K traces by fitting an exponential to the rising phase of the inward current and subtracting this waveform from each record. (*B*) Results from an analogous experiment with an oocyte expressing sqKv1A channels. These records represent the first pulse in 4AP after a wait of 5–7 min. (*C*) I_K records for sqKv1A channels are illustrated after achieving maximal 4AP-block as described in the text. (*D*) Hill-plot analysis of data from GFL neurons (*filled symbols*) and oocytes expressing sqKv1A. Open squares are from resting sqKv1A channels (first pulse; see *B*); open circles are for activated channels (maximal block; see *C*). GFL data are either pooled from a number of different neurons (▲) or are from a single cell (■). Oocyte data represent means ± SD ($n = 3$). Approximate K_d values are 5 μM for native g_K, 75 μM for activated sqKv1A, and >3 mM for resting sqKv1A. Solid lines are least-square fits. Slopes for GFL and activated sqKv1A are ~1; slope for resting sqKv1A is 0.85.

heterologously expressed sqKv1A channels versus the native "delayed-rectifier" g_K in squid GFL neurons and giant axons. Furthermore, we find that 4AP displays greatly different affinities for sqKv1A and native channels when they are in the resting state. All of these functional discrepancies implicate structural differences in the external and internal mouths of the pore. We are unaware of examples of any post-translational modifications that produce such effects, and consider such hypothetical modifications to be unlikely.

Taken together, these findings do not support the idea that the native channel in the giant-axon/GFL system is a homotetramer composed of sqKv1A α-subunits. Although we cannot at present account for the mechanistic origin of the observed differences, much has been learned from the journey.

C-type inactivation of sqKv1A channels

Pharmacological results from *Xenopus* oocytes and *Sf*9 cells suggest that sqKv1A channels inactivate by a C-type mechanism like that found in *Shaker* B and other Kv1 channels. This assertion was substantiated by mutational analyses in the present study. Deletion of the amino-terminus nearly to the start of the T1 domain has no apparent affect on inactivation, making a conventional N-type mechanism highly improbable. Molecular rearrangements underlying C-type inactivation involve many residues of the turret-pore region (Yellen, 1998; Gandhi et al., 2000; Larsson and Elinder, 2000), and several positions are particularly critical. One of these, residue 449 of *Shaker* B, flanks the outer mouth of the pore (Doyle et al., 1998), and substitution of the wild-type threonine (T449) with serine (T449S) or valine (T449V) substantially accelerates or impedes inactivation, respectively (Schlief et al., 1996; Lopez-Barneo et al., 1993). Inactivation of sqKv1A channels shows the same pattern in comparing wild-type serine at the homologous position (S375) with the mutations S375T and S375V.

We have identified another position that is equally critical to inactivation of sqKv1A channels. Substitution of histidine 351 (H351) with a variety of amino acids profoundly affects inactivation. Rates of inactivation for these mutants show a positive correlation with the rate of I_K rundown induced by Chl-T, similar to the pattern found with T449 mutations in *Shaker* B (Schlief et al., 1996). This implicates H351 with a C-type inactivation mechanism in sqKv1A, and the analogous residue in *Shaker* B (F425) is also probably important (Perez-Cornejo, 1999).

Mutations at this turret position, at least in sqKv1A, can clearly dominate the influence of the critical residue Ser-375 (Thr-449 of *Shaker* B) on inactivation kinetics. This feature allows controlled manipulation of C-type inactivation kinetics without directly altering critical residues in the external mouth of the pore, and such an ability may be useful in future studies of the role of permeating and blocking ions in C-type inactivation.

Analysis of inactivation kinetics for the series of H351 mutants reveals a general trend in which charged and small, hydrophobic residues at this position disrupt inactivation, and large aromatic residues accelerate it (Fig. 4 *A*). Wild-type histidine presents an exception to this generalization, however, because inactivation is faster at low pH when H351 would be expected to be charged (unpublished data). Difficulty in drawing a definitive correlation between amino

acid side chain structure and inactivation rate probably reflects the complex and relatively large-scale molecular motions involved in C-type inactivation.

Effects of external TEA and K^+ ions on inactivation of sqKv1A versus native K^+ channels

Properties of native channels in GFL neurons differ significantly from those of sqKv1A in regard to the effects of external TEA and K^+ ions on inactivation. Neither external TEA nor K^+ slows inactivation of the native channel (Mathes et al., 1997; Brock et al., 2001), whereas both agents do so in the case of sqKv1A. This qualitative difference is not due to the different ionic conditions (i.e., ionic strength; divalent cation or potassium concentrations) in the experimental solutions used for GFL neurons versus amphibian or insect heterologous expression systems (Brock et al., 2001 and unpublished data).

The inability of TEA to slow inactivation does not preclude a C-type mechanism in the native channels, however. External TEA does not slow rapid C-type inactivation in *Shaker* B channels with certain mutations in the outer mouth of the pore (e.g., T449K; Molina et al., 1997). Although such a situation might well occur in the native squid channel, it is difficult to see how it would arise if the channels were composed of sqKv1A homotetramers.

External K^+ ions also slow C-type inactivation, at least in Kv1 channels showing rapid inactivation in low K^+, and this effect appears to be universal in cloned Kv1 channels (Yellen, 1998). In *Shaker* B, K^+ ions appear to interact with the inactivation mechanism through occupancy of a binding site located between positions T441 and T449 in the primary sequence (Baukrowitz and Yellen, 1996; Harris et al., 1998). Amino acids at these nine positions are universally conserved in Kv1 α-subunits, but how occupancy of this K^+-binding site is coupled to movements of residues that influence C-type inactivation is not known.

High external K^+ does alter inactivation of both native and sqKv1A channels in one qualitatively similar way. Inactivation is incomplete in both channel types, and the fraction of non-inactivating I_K increases in elevated K^+ concentrations (Fig. 2 *D* of this paper and Fig. 11 *A* of Mathes et al., 1997). Thus, permeating K^+ ions appear to stabilize the open state in the native channel and in sqKv1A and other Kv1 members, but the precise mechanisms coupling K^+ occupancy to inactivation kinetics must still differ in some way.

Differential effects of Chl-T on I_K from native and sqKv1A channels

Chl-T oxidizes methionine and cysteine residues. In *Shaker* B $\Delta 6-46$ acceleration of inactivation by Chl-T has been attributed to oxidation of Met-448 in the outer mouth of the pore (Schlief et al., 1996), but other unidentified residues are also involved in the rundown phenomenon. Our data for sqKv1A showing different rates for the appearance of the rapidly inactivating component of I_K and for the loss of I_K are consistent with this position.

Treatment with Chl-T does not accelerate inactivation of the native channel in a comparable way, and actually reduces the amount of rapidly inactivating I_K in relation to the non-inactivating component. This results in an overall slowing of inactivation in GFL cells after Chl-T treatment, and inactivation kinetics after treatment remain insensitive to external TEA and K^+ ions (unpublished data). Thus, Chl-T treatment does not confer sqKv1A-like properties to native channels. Alternatively, it could be argued that oxidation of M374 of sqKv1A (equivalent to M448 in *Shaker* B) by Chl-T induces a biphasic inactivation process that is similar to that seen with native I_K. This similarity is likely to be superficial, however, because kinetics of sqKv1A channels remain sensitive to external K^+ after treatment with Chl-T (unpublished data).

At present, the significance of the contrasting effects of Chl-T on inactivation kinetics in native versus sqKv1A remains unclear. Presumably, Chl-T is able to oxidize the relevant methionine residue (universally conserved in Kv1 members) in both cases, but the molecular mechanisms that couple this event to other residues controlling C-type inactivation would appear to differ. The complex effects of Chl-T and multiple sites of action make speculation concerning such differences premature.

Differential state-dependencies of block by 4AP

In squid giant axons and GFL neurons, 4AP blocks resting channels at very negative holding potentials, and block is rapidly relieved by strong depolarization (Yeh et al., 1976; Kirsch and Narahashi, 1983; Kirsch et al., 1986; this study). 4AP is a poor blocker of resting sqKv1A channels, and activation dramatically enhances block. In this case, 4AP appears to remain "trapped" in its blocking position following repolarization (Armstrong and Loboda, 2001).

These observations suggest the observed state-dependencies of 4AP block may be a product of differential accessibility of the 4AP binding site. However, it is difficult to rule out a difference in spontaneous openings at highly negative voltages in the two channel types as a contributing factor. Although we do not have accurate measurements of open probability for either channel type at -80 to -100 mV, the similarity of the macroscopic g_K-V relations (Brock et al., 2001) suggest that it must be extremely low in both cases. It seems unlikely that this factor alone could account for the potent block of resting native channels at -80 mV by 0.1 mM 4AP (Fig. 9 *B*) and essentially no block under similar conditions with sqKv1A.

To our knowledge, all other Kv1 homotetramers show the sqKv1A-type of pattern for 4AP block (McCormack et al.,

1994; Stephens et al., 1994; Russell et al., 1994; Yao and Tseng, 1994; Yamane et al., 1995) as do native channels in lymphocytes (Kv1.3; Choquet and Korn, 1992). A similar situation exists with Kv2.1 (Kirsch and Drewe, 1993). However, Kv3.1 (Kirsch and Drew; 1993) and Kv4 members (Tseng et al., 1996; Jerng et al., 1999) show "resting-channel" block, as does the putative native Kv4 channel responsible for calcium-independent transient outward K^+ current (I_{to}) in ventricular myocytes (Campbell et al., 1993).

It is presently unclear what gives rise to these differences. Mutagenesis studies with Kv2.1 and Kv3.1 (Kirsch et al., 1993) suggest that 4AP interacts with residues localized to the cytoplasmic halves of transmembrane segments S5 and S6. The relevant S6 residues correspond to positions 469–476 of *Shaker* B, and this short stretch of amino acids straddles a pair of prolines (P473 and P475 in *Shaker* B) near the intracellular end of the pore (Doyle et al., 1998) that may be intimately involved with activation gating (Liu et al., 1997; Yellen, 1998). Although it is likely that this region of the inner pore is involved in state-dependent block by 4AP, mechanistic details and the role of S5 residues are presently unknown.

Implications for the molecular identification of squid and other native K^+ channels

Voltage-gated channels are multi-subunit, integral membrane proteins and are thus exposed to a variety of extracellular and cytoplasmic factors and elements in the lipid bilayer. Biophysical and pharmacological properties of these channels are defined largely, but no means entirely, by the four α-subunits that form the channel proper. Heteromultimers may form by combination of different α-subunits belonging to the same subfamily, e.g., Kv1 (Covarrubias et al., 1991; Li et al., 1992; Xu et al., 1995), and specific functional properties of heteromultimers can be different than those in the corresponding homotetramers (Rupersberg et al., 1990; Isacoff et al., 1990) and are usually intermediate in nature (MacKinnon, 1991; MacKinnon et al., 1993).

Discrepancies between inactivation properties of native K^+ channels in GFL neurons and sqKv1A homotetramers in oocytes as described in this paper consistently implicate structural features in the outer mouth of the conducting pore. Primary determinants of the relevant properties are thought to be specific residues on the Kv1 α-subunits themselves. We therefore favor the idea that the native squid channel in question is formed by sqKv1A α-subunits in combination with another squid Kv1 member that confers a unique set of properties to the heteromultimers.

It is particularly surprising that the native channels do not show the "standard" Kv1-type of 4AP sensitivity, i.e., poor block under resting conditions. However, the cited studies were all carried out on Kv1 homotetramers, and 4AP block of heteromultimers has not been extensively studied. It is extremely unlikely that the native squid channel is actually a Kv3 or Kv4 member that is sensitive to 4AP at rest. The sensitivity of native channels to *S*-nitrosodithiothreitol (a Kv1-specific blocker; Brock and Gilly, 2001), the pH-dependence of block by tityustoxin-Kα (Ellis et al., 2001), and substantial molecular and biochemical evidence (see Introduction) provide compelling evidence that the native channel is a Kv1 type. However, preliminary evidence has revealed another squid Kv1 α-subunit expressed in the giant fiber lobe that is not sensitive to tityustoxin or external TEA (Jerng et al., 2001), potentially consistent with the heteromultimer hypothesis. Present work is directed at exploring this possibility. An alternative idea that the native squid channel is a heteromultimer of sqKv1A and a squid Kv3 or Kv4 member has no foundation in the literature whatsoever.

In reality, actual structural differences present in a squid Kv1 heteromultimer need not be major to account for observed functional discrepancies. For example, inactivation in the presence of TEA could occur from a partially activated but closed state or from a blocked state more readily in the native channels than in sqKv1A. Such behavior would be consistent with the prominent flickering characteristic of single channel activity of both channel types (Perozo et al., 1991; Nealey et al., 1993; Rosenthal et al., 1996). This might mask the effect of TEA on inactivation kinetics in native channels (see also Jerng and Covarrubias, 1997; Jerng et al., 1999), even though the relevant structural difference might be subtle.

Equating a cloned channel with its supposed native counterpart necessitates stringent comparisons of both functional and pharmacological characteristics. The native channel can be indicated to be a homotetramer composed of a specific α-subunit only when a suite of these properties is closely matched. Exactly how close this match needs to be to make a definitive conclusion is difficult to define. Formation of heteromultimeric channels in native tissues greatly complicates such identifications, however, and rigorous functional comparison of channels in heterologous expression systems and in native neurons remains challenging.

We thank Dr. T. I. Liu for conducting some experiments and Jeni Boustani for generating several of the H351 mutants described in this paper. We are also grateful to Dr. Manuel Covarrubias for critical reading of this manuscript.

This work was supported by National Institutes of Health Grant NS-17510.

REFERENCES

Armstrong, C. M. 1969. Inactivation of the potassium conductance and related phenomena caused by quaternary ammonium ion injection in squid axons. *J. Gen. Physiol.* 54:553–575.

Armstrong, C. M., and F. Bezanilla. 1973. Currents related to movement of the gating particles of the sodium channel. *Nature.* 242:459–461.

Armstrong, C. M., and A. Loboda. 2001. A model for 4-aminopyridine action on K^+ channels: similarities to tetraethylammonium ion action. *Biophys. J.* 81:895–904.

Baukrowitz, T., and G. Yellen. 1995. Modulation of K^+ current by frequency and external [K^+]: a tale of two inactivation mechanisms. *Neuron.* 15:951–960.

Baukrowitz, T., and G. Yellen. 1996. Use-dependent blockers and exit rate of the last ion from the multi-ion pore of a K^+ channel. *Science.* 271:653–656.

Brock, M. W., Z. N. Lebaric, H. Neumeister, A. DeTomaso, and W. F. Gilly. 2001. Temperature-dependent expression of a squid Kv1 channel in Sf9 cells and functional comparison with the native delayed rectifier. *J. Membr. Biol.* 180:147–161.

Campbell, D. L., Y. Qu, R. L. Rasmusson, and H. C. Strauss. 1993. The calcium-independent transient outward potassium current in isolated ferret right ventricular myocytes. *J. Gen. Physiol.* 101:603–626.

Choi, K. L., R. W. Aldrich, and G. Yellen. 1991. Tetraethylammonium blockade distinguishes two inactivation mechanisms in voltage-activated K^+ channels. *Proc. Natl. Acad. Sci. U.S.A.* 88:5092–5095.

Choquet, D., and H. Korn. 1992. Mechanism of 4-aminopyridine action on voltage-gated potassium channels in lymphocytes. *J. Gen. Physiol.* 99: 217–240.

Covarrubias, M., A. A. Wei, and L. Salkoff. 1991. *Shaker*, *Shal*, *Shab*, and *Shaw* express independent K^+ current systems. *Neuron.* 7:763–773.

Doyle, D. A., J. M. Cabral, R. A. Pfuetzner, A. Kuo, J. Gulbis, S. Cohen, B. T. Chait, and R. MacKinnon. 1998. The structure of the potassium channel: molecular basis of potassium conduction and selectivity. *Science.* 280:69–77.

Ellis, K. C., H. Tenenholz, H. H. Jerng, M. Hayhurst, C. S. Dudlak, W. F. Gilly, M. P. Blaustein, and D. J. Weber. 2001. Interaction of a toxin from the scorpion *Tityus serrulatus* with a cloned K^+ channel from squid (sqKv1A). *Biochemistry.* 40:5942–5953.

Gandhi, C. S., E. Loots, and E. Y. Isacoff. 2000. Reconstructing voltage sensor-pore interaction from a fluorescence scan of a voltage-gated K^+ channel. *Neuron.* 27:585–595.

Gilly, W. F., M. T. Lucero, and F. T. Horrigan. 1990. Control of the spatial distribution of sodium channels in giant fiber lobe neurons of the squid. *Neuron.* 5:663–674.

Grissmer, S., and M. Cahalan. 1989. TEA prevents inactivation while blocking open K^+ channels in human T lymphocytes. *Biophys. J.* 55:203–206.

Harris, R. E., H. P. Larsson, and E. Y. Isacoff. 1998. A permeant ion binding site located between two gates of the *Shaker* K^+ channel. *Biophys. J.* 74:1808–1820.

Hodgkin, A. L., and A. F. Huxley. 1952. A quantitative description of membrane current and its application to conduction and excitation in nerve. *J. Physiol.* 117:500–544.

Hoshi, T., W. N. Zagotta, and R. W. Aldrich. 1990. Biophysical and molecular mechanisms of *Shaker* potassium channel inactivation. *Science.* 250:533–538.

Isacoff, E. Y., Y. N. Jan, and L. Y. Jan. 1990. Evidence for the formation of heteromultimeric potassium channels in *Xenopus* oocytes. *Nature.* 345:530–534.

Iverson, L. E., and B. Rudy. 1990. The role of divergent amino and carboxyl domains on the inactivation properties of potassium channels derived from the *Shaker* gene of *Drosophila*. *J. Neurosci.* 10: 2903–2916.

Jerng, H. H., J. Beerman, J. J. C. Rosenthal, and W. F. Gilly. 2001. Two types of Kv1 α-subunits may contribute to properties of native channels in the squid giant axon system. *Biophys. J.* 80:434*a*. (Abstr.).

Jerng, H. H., and M. Covarrubias. 1997. K^+ channel inactivation mediated by the concerted action of the cytoplasmic N- and C-terminal domains. *Biophys. J.* 72:163–174.

Jerng, H. H., and W. F. Gilly. 1999. C-type inactivation of a cloned squid K^+ channel expressed in *Xenopus* oocytes. *Biophys. J.* 76:191*a*. (Abstr.).

Jerng, H. H., M. Shahidullah, and M. Covarrubias. 1999. Inactivation gating of Kv4 potassium channels: molecular interactions involving the inner vestibule of the pore. *J. Gen. Physiol.* 113:641–660.

Kirsch, G. E., and J. A. Drewe. 1993. Gating-dependent mechanism of 4-aminopyridine block in two related potassium channels. *J. Gen. Physiol.* 102:797–816.

Kirsch, G. E., and T. Narahashi. 1983. Site of action and active form of aminopyridine in squid axon membranes. *J. Pharmacol. Exp. Ther.* 226:174–179.

Kirsch, G. E., C-C. Shieh, J. A. Drewe, D. F. Vener, and A. M. Brown. 1993. Segmental exchanges define 4-aminopyridine binding and the inner mouth of K^+ pores. *Neuron.* 11:503–512.

Kirsch, G. E., J. Z. Yeh, and G. S. Oxford. 1986. Modulation of aminopyridine block of potassium currents in squid axon. *Biophys. J.* 50: 637–644.

Larsson, H. P., and F. Elinder. 2000. A conserved glutamate is important for slow inactivation in K^+ channels. *Neuron.* 27:573–583.

Li, M., Y. N. Jan, and L. Y. Jan. 1992. Specification of subunit assembly by the hydrophilic amino-terminal domain of the *Shaker* potassium channel. *Science.* 257:1225–1229.

Liu, Y., M. Holmgren, M. E. Jurman, and G. Yellen. 1997. Gated access to the pore of a voltage-dependent K^+ channel. *Neuron.* 19:175–184.

Liu, T. I., Z. Lebaric, J. J. C. Rosenthal, and W. F. Gilly. 2001. Natural substitutions at highly conserved T1-domain residues perturb processing and functional expression of squid Kv1 channels. *J. Neurophysiol.* 85:61–71.

Llano, I., and R. J. Bookman. 1986. Ionic conductances of squid giant fiber lobe neurons. *J. Gen. Physiol.* 88:543–569.

Llano, I., C. K. Webb, and F. Bezanilla. 1988. Potassium conductance of the squid giant axon: single channel studies. *J. Gen. Physiol.* 92: 179–196.

Lopez-Barneo, J., T. Hoshi, S. H. Heinemann, and R. W. Aldrich. 1993. Effects of external cations and mutations in the pore region on C-type inactivation of *Shaker* potassium channels. *Rec. and Chann.* 1:61–71.

MacKinnon, R. 1991. Determination of the subunit stoichiometry of a voltage-activated potassium channel. *Nature.* 350:232–235.

MacKinnon, R., R. W. Aldrich, and A. W. Lee. 1993. Functional stoichiometry of *Shaker* potassium channel inactivation. *Science.* 262:757–759.

Mathes, C., J. J. C. Rosenthal, C. M. Armstrong, and W. F. Gilly. 1997. Fast inactivation of delayed rectifier K^+ conductances in squid giant axon and cell bodies. *J. Gen. Physiol.* 109:435–448.

McCormack, K., W. J. Joiner, and S. H. Heinemann. 1994. A characterization of the activating structural rearrangements in voltage-dependent *Shaker* K^+ channels. *Neuron* 12:301–315.

McFarlane, M. B., and W. F. Gilly. 1996. Spatial localization and omega-Agatoxin block of calcium channels in giant fiber lobe neurons of the squid *Loligo opalescens*. *Proc. Natl. Acad. Sci. U.S.A.* 93:5067–5071.

Molina, A., A. G. Castellano, and J. Lopez-Barneo. 1997. Pore mutations in *Shaker* K^+ channels distinguish between the sites of tetraethylammonium blockade and C-type inactivation. *J. Physiol.* 499:361–367.

Nealey, T., S. Spires, R. A. Eatock, and T. Begenisich. 1993. Potassium channels in squid neuron cell bodies: comparison to axonal channels. *J. Membr. Biol.* 132:13–25.

Perez-Cornejo, P. 1999. H^+ ion modulation of C-type inactivation of *Shaker* K^+ channels. *Pflugers Arch.- Eur. J. Physiol.* 437:865–870.

Perez-Cornejo, P., P. Stampe, and T. Begenisich. 1998. Proton probing of the charybdotoxin binding site of *Shaker* K^+ channels. *J. Gen. Physiol.* 111:441–450.

Perozo., E., D. S. Jong, and F. Bezanilla. 1991. Single channel studies of the phosphorylation of K^+ channels in the squid giant axon. II. Nonstationary conditions. *J. Gen. Physiol.* 98:19–34.

Rosenthal, J. J. C., T. I. Liu, and W. F. Gilly. 1997. A family of delayed rectifier Kv1 cDNAs showing cell type-specific expression in the squid stellate ganglion/giant fiber lobe complex. *J. Neurosci.* 17:5070–5079.

Rosenthal., J. J. C., R. G. Vickery, and W. F. Gilly. 1996. Molecular identification of sqKv1A: a candidate for the delayed rectifier K^+ channel in squid giant axon. *J. Gen. Physiol.* 108:207–219.

Ruppersberg, J. P., K. H. Schruter, B. Sakmann, M. Stocker, S. Sewing, and O. Pongs. 1990. Heteromultimeric channels formed by rat brain potassium channel proteins. *Nature* 345:535–537.

Russell, S. N., N. G. Publicover, P. J. Hart, A. Carl, J. R. Human, K. M. Sanders, and B. Horowitz. 1994. Block by 4-aminopyridine of a Kv1.2 delayed rectifier K^+ current expressed in *Xenopus* oocytes. *J. Physiol.* 481:571–584.

Schlief, T., R. Schonherr, and S. H. Heinemann. 1996. Modification of C-type inactivating *Shaker* potassium channels by chloramine-T. *Pflugers Arch.- Eur. J. Physiol.* 431:483–493.

Stephens, G. J., J. C. Garratt, B. Robertson, and D. G. Owen. 1994. On the mechanism of 4-aminopyridine action on the cloned mouse brain potassium channel mKv1.1. *J. Physiol.* 477:187–196.

Thompson, J., and T. Begenisich. 2000. Electrostatic interaction between charybdotoxin and a tetrameric mutant of *Shaker* K^+ channels. *Biophys. J.* 78:2382–2391.

Tseng, G-N., M. Jiang, and J-A. Yao. 1996. Reverse use dependence of Kv4.2 blockade by 4-aminopyridine. *J. Pharmacol. Exp. Ther.* 279: 865–876.

Xu, J., W. Yu, Y. N. Jan, L. Y. Jan, and M. Li. 1995. Assembly of voltage-gated potassium channels: conserved hydrophilic motifs determine subfamily-specific interactions between the α-subunits. *J. Biol. Chem.* 270:24761–24768.

Yamane, T., T. Furukawa, and M. Hiraoka. 1995. 4-Aminopyridine block of the noninactivating cloned K^+ channel Kv1.5 expressed in *Xenopus* oocytes. *Am. J. Physiol. Heart Circ. Physiol.* 269:H556–H564.

Yao, J-A., and G-N. Tseng. 1994. Modulation of 4AP block of a mammalian A-type K^+ channel clone by channel gating and membrane voltage. *Biophys. J.* 67:130–142.

Yeh, J. Z., G. S. Oxford, C. H. Wu, and T. Narahashi. 1976. Dynamics of aminopyridine block of potassium channels in squid axon membrane. *J. Gen. Physiol.* 68:519–535.

Yellen, G. 1998. The moving parts of voltage-gated ion channels. *Q. Rev. Biophys.* 31:239–295.